ELSEVIER

Journal of Nuclear Materials 294 (2001) 1–7

journal of nuclear materials

www.elsevier.nl/locate/jnucmat

Section 1. Fuel behaviour and processes

Heat capacity measurements on unirradiated and irradiated fuel pellets

Masaki Amaya [a,*,1], Katsumi Une [a,1], Kazuo Minato [b]

[a] *Nippon Nuclear Fuel Development Co., Ltd., 2163 Narita-cho, Oarai-machi, Higashi-ibaraki-gun, Ibaraki-ken 311-1313 Japan*
[b] *Japan Atomic Energy Research Institute Tokai-mura, Naka-gun, Ibaraki-ken 319-1195, Japan*

Abstract

Heat capacities (C_p) of oxide fuels are essential for the evaluation of fuel temperature at normal, transient and accidental conditions of light water reactors. In this study, the effect of soluble fission products (FPs) was first examined, and then the C_p measurement technique was improved to obtain reliable data for irradiated pellets of smaller than the standard size. A differential scanning calorimeter was applied to the C_p measurements. From the measurements of standard size α-Al_2O_3, the inaccuracy of the apparatus was estimated to be about 4%. The C_p data of undoped and simulated FPs-doped UO_2 pellets of standard size were measured in the temperature region from 325 to 1673 K. From these results, the effect of impurities on the C_p values of UO_2 pellets and the presence of the C_p anomalies in the simulated FPs-doped UO_2 pellets were investigated. For measurements of small size specimens, the sample-side crucible was modified. The inaccuracy of the apparatus was estimated to be 5% using a small size of the α-Al_2O_3 sample. This improved technique was applied to obtain the C_p data of UO_2 and UO_2–10 wt%Gd_2O_3 specimens with small sizes from 325 to 1673 K, which had been irradiated at isothermal conditions in a test reactor.

1. Introduction

The temperature of nuclear fuel pellets is one of the most important factors that control the behavior of fission products (FPs) in the pellets, the diffusion and vaporization properties and so on. The pellet temperature is controlled by the pellet specific heat capacity as well as their thermal conductivity, and the specific heat capacity of the fuel pellets at high-temperature is necessary to estimate the temperature changes under normal and accidental reactor conditions.

Heat capacities of undoped and impurity-doped UO_2 pellets have been measured by many researchers [1–15]. While the heat capacities of undoped UO_2 pellets were in good agreement with each other, the heat capacities of impurity-doped UO_2 pellets showed large scatter between literature data: two groups [6,11–13] have reported high-temperature heat capacity anomalies for Gd_2O_3-doped and simulated FPs-doped UO_2 pellets. On the other hand, two other groups [7–9,14,15,27] observed no heat capacity anomalies of impurity-doped UO_2 pellets. Also, studies on the effects of irradiation on the heat capacity of fuel pellets are few in number.

Recently, Gomme et al. [16] measured the specific heat capacities of irradiated UO_2 pellets. They observed a decrease of specific heat capacity and hysteresis in the data above 900 K. However, they did not evaluate the effects of irradiation on the heat capacity of fuel pellets, and their data showed a large scattering while the estimated inaccuracy of their apparatus was about 10%. Therefore, in order to evaluate the effects of irradiation on the heat capacity in detail, it is necessary to develop a measurement technique for heat capacity of irradiated fuel pellets having a small size.

In this paper, first, heat capacities of unirradiated fuel pellets, such as undoped UO_2 and simulated soluble

* Corresponding author. Tel.: +81-29 267 9011; fax: +81-29 267 9014.
E-mail address: amaya@nfd.co.jp (M. Amaya).
[1] Present address: Japan Nuclear Fuel Co., Ltd., 2163 Narita-cho, Oarai-machi, Higashi-ibaraki-gun, Ibaraki-ken 311-1313, Japan.

0022-3115/01/$ - see front matter
PII: S0022-3115(01)00450-0

FPs-doped fuel pellets were measured by using standard size samples. Based on the measured heat capacities, their anomalies at high-temperature and the effects of soluble impurities on the heat capacity of fuel pellets were investigated. Second, the heat capacity measurement technique was developed for irradiated fuel samples having smaller sizes than the standard samples. The technique was applied to measure the heat capacities from 325 to 1673 K of fuel pellets irradiated in a test reactor.

2. Experimental

2.1. Sample preparation for unirradiated fuel pellets

Characteristics of the unirradiated samples for heat capacity measurements are summarized in Table 1. Slices were prepared from the pellet (10 mm diameter and 10 mm height) which had been sintered at 2023 K for 4 h in N_2–8% H_2 atmosphere. No microcracks were observed in the sintered pellets by ceramography. Samples for heat capacity measurements were cut from the slices by using an ultrasonic cutter. Each sample was 5.2 mm diameter and 1 mm thickness and weighed about 200 mg.

2.2. Sample preparation for irradiated fuel pellets

Characteristics of the samples for heat capacity measurements are shown in Table 2. The samples (regular prism (square) with a 2.4 mm side and 1 mm thickness or circular disk with a 2.6 mm diameter and 1 mm thickness) were sandwiched between molybdenum disks and they were inserted into fuel pins. The fuel pins were placed into capsules and irradiated in a test reactor (JRR-3, Japan Atomic Energy Research Institute) under isothermal conditions. The irradiation temperatures were from 873 to 1273 K and some samples experienced temperature above 1273 K in the last period of irradiation. Example ceramographs of samples, which experienced these high-temperatures are shown in Fig. 1. Structural changes were observed in them due to fission gas release.

The masses for heat capacity measurements were from 40 to 60 mg. Differences of sample masses before and after heat capacity measurements were negligible. No cracks and chips were observed in the samples after heat capacity measurements.

2.3. Heat capacity measurements

Heat capacities of unirradiated and irradiated fuel pellets were measured by using a differential scanning calorimeter (DSC: Netzsch DSC-404, high-temperature type). A schematic diagram of the apparatus is shown in Fig. 2. A sample was set in an alumina-lined platinum crucible on the sample side of the heat flux sensor in a measuring head. A platinum sheet was placed on the sample in order to reduce the effects of radiation from it on the heat capacity measurements. For an irradiated sample, a platinum washer was also set in the sample side crucible to prevent sample position changes during measurements. The flow-type ionization chamber was

Table 1
Sample characteristics of unirradiated fuel pellets for heat capacity measurements

Sample no.	Simulated burnup (GWd/t)	Impurity content (at.%)								Formula weight	Sample mass (g)	Mole number ($\times 10^{-4}$ mol)
		Gd	Sr	Zr	Y	La	Ce	Nd	Total			
1	0	0	0	0	0	0	0	0	0	270.03	0.2228	8.251
2	30	0	0.23	0.87	0.12	0.19	0.63	0.63	2.68	266.78	0.2112	7.917
3	90	0	0.47	2.15	0.24	0.54	1.66	1.90	6.95	261.86	0.2237	8.543
4	30	8.72	0.21	0.80	0.11	0.18	0.58	0.58	11.2	259.95	0.2206	8.486

Table 2
Sample characteristics of irradiated fuel pellets for heat capacity measurements

Sample no.	Burnup (GWd/t)	Irradiation temperature (K)	Sample size[a]	Gd_2O_3 content (wt%)	Sample mass[b] (mg)
D14	39	873[c]	a	0	60.0
F14	40	873[c]	a	10	57.4
G4	45	1123–1273	b	0	42.4

[a] a: Square with a 2.4 mm side and 1 mm thickness; b: circular with a 2.6 mm diameter and 1 mm thickness.
[b] Changes of the sample masses during heat capacity measurements were negligible.
[c] Samples experienced temperatures above 1273 K in the last period of irradiation.

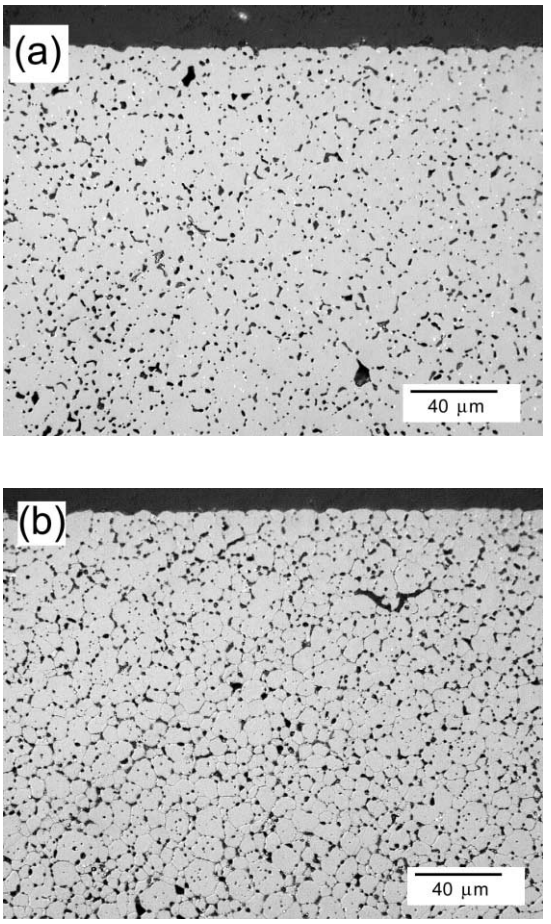

Fig. 1. Example ceramographs of irradiated UO_2 pellet for heat capacity measurements: (a) as-polished; (b) as-etched.

connected to the gas outlet of the DSC apparatus in order to monitor the β activities of released ^{85}Kr from samples continuously. The reducing gas of argon containing 0.2% hydrogen was introduced into the measuring part of apparatus to prevent sample oxidation during heat capacity measurements. The gas flow rate was 50 ml min^{-1}. The temperature-scanning speed was 20 K min^{-1} and the temperature range was from 325 to 1673 K.

In order to check the accuracy of the apparatus, the molar heat capacities of α-Al_2O_3 (standard size: 5.2 mm diameter and 1 mm thickness) were measured and are shown in Fig. 3. Literature data obtained by Archer [17] are also shown for comparison. Based on this, the accuracy of the apparatus used in this study was estimated to be ±4%.

A small sample of α-Al_2O_3 (microsample size: square with a 2.5 mm side and 1 mm thickness) was used to estimate the accuracy of the apparatus for microsamples. The measured heat capacities of microsample size

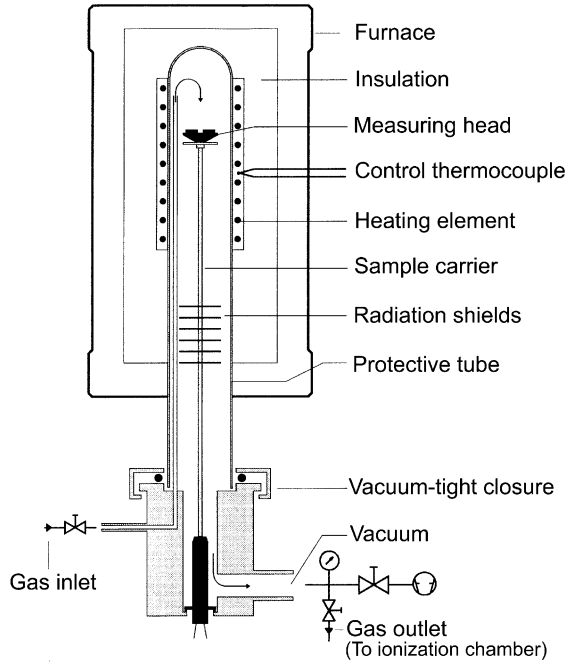

Fig. 2. Schematic diagram of the apparatus for heat capacity measurements.

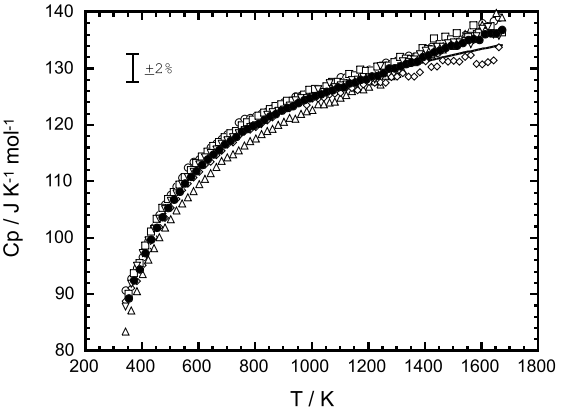

Fig. 3. Heat capacities of α-Al_2O_3 (standard size: 5.2 mm diameter and 1 mm thickness). ○: measurement 1; △: measurement 2; □: measurement 3; ◇: measurement 4; ▽: measurement 5; ●: averaged values of measurement 1–5; ——: Archer [17].

α-Al_2O_3 were shown in Fig. 4 along with literature data [17] and the standard size results. While the scattering between the measurement values became larger with increasing temperature, the accuracy of the apparatus was estimated to be 5% for the microsample under 1400 K. This fact means that the microsample heat capacity can be measured within nearly the same error as that of the standard size by applying the improved technique as described above.

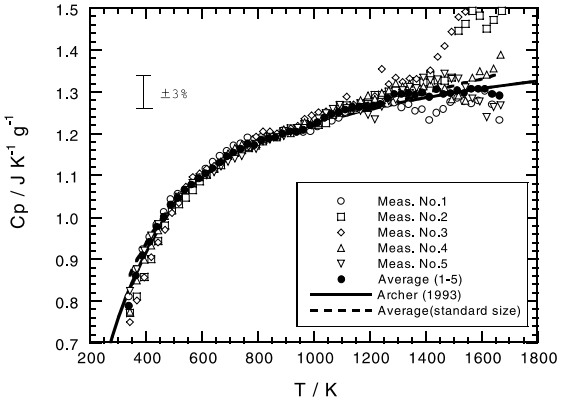

Fig. 4. Heat capacities of α-Al_2O_3 (microsample: square with a 2.5 mm side and 1 mm thickness). ○: measurement 1; △: measurement 2; □: measurement 3; ◇: measurement 4; ▽: measurement 5; ●: averaged values of measurement 1–5; – – – –: averaged values for standard size; ———: Archer [17].

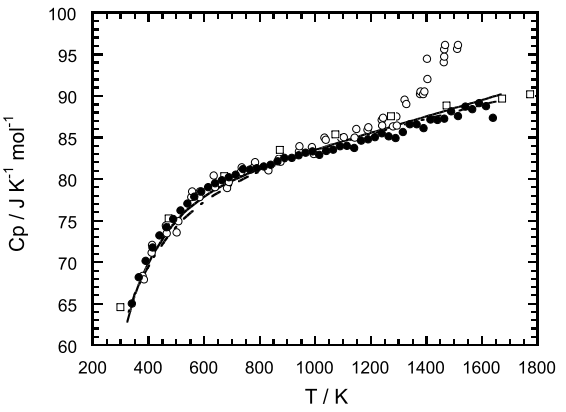

Fig. 6. Heat capacities of simulated FPs-doped UO_2 (simulated burnup: 30 GWd/t). ●: this work; ○: Arita et al. [11] (simulated burnup: 19 GWd/t); □: Lucuta et al. [14] (simulated burnup: 28 GWd/t); ———: undoped UO_2 (this work); — · —: values evaluated from summation rule (Neumann–Kopp's law).

3. Results and discussion

3.1. Heat capacities of unirradiated fuel pellets

The results of molar heat capacities of undoped UO_2 are shown in Fig. 5. The measured molar heat capacities are in good agreement with other literature data [1–7,11], within the experimental error of this study (±2%).

The molar heat capacities of simulated soluble FPs-doped UO_2 (simulated burnup: 30 GWd/t and 90 GWd/t) are shown in Figs. 6 and 7. The measured heat capacities are close to the values calculated from the summation rule by using heat capacity data of soluble FPs [18]. No anomalous increase of heat capacities was

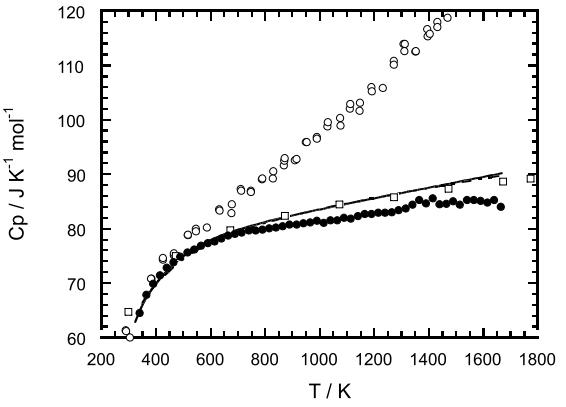

Fig. 7. Heat capacities of simulated FPs-doped UO_2 (simulated burnup: 90 GWd/t). ●: this work; ○: Arita et al. [11] (simulated burnup: 94 GWd/t); □: Lucuta et al. [14] (simulated burnup: 75 GWd/t); ———: undoped UO_2 (this work); — · —: values evaluated from summation rule (Neumann–Kopp's law).

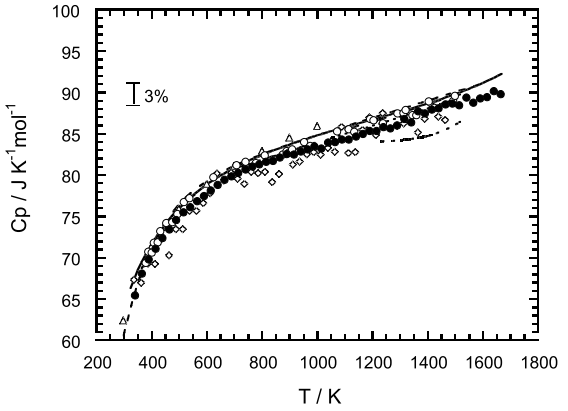

Fig. 5. Heat capacities of undoped UO_2. ●: this study; ———: MATPRO [1]; — · —: Grønvold et al. [2]; — — ·: Kerrisk and Clifton [3]; .....: Fredrickson and Chasanov [4]; — · · — · —: Hein et al. [5]; ○: Inaba et al. [6]; △, ◇: Takahashi and Asou [7]; – – – – –: Arita et al. [11].

observed in the temperature range above 1000 K, which is in contrast with the results reported by Arita and coworkers [11–13]. The measured heat capacities of other impurity-doped UO_2 pellets (Gd_2O_3 content: 6 wt%, simulated burnup: 30 GWd/t) have similar tendencies to those of the 30 GWd/t-simulated UO_2 pellets as shown in Fig. 8.

The measured molar heat capacities were fitted to the following equation:

$$C_p = a + bT + C/T^2, \tag{1}$$

where C_p is the molar heat capacity in J K^{-1} mol^{-1}; a, b and c are the fitting parameters; and T is the temperature in K. The fitting results are summarized in Table 3.

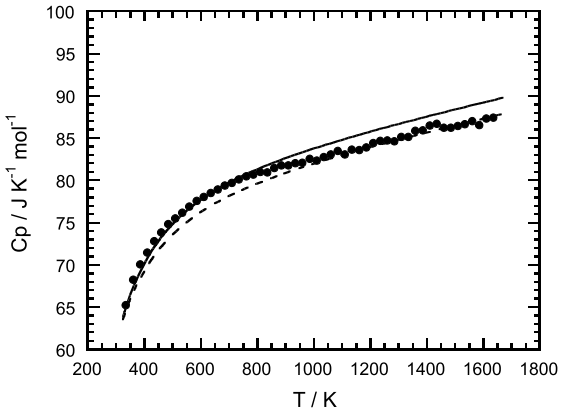

Fig. 8. Heat capacities of simulated FPs-doped UO_2 (6 wt% Gd_2O_3-doped, simulated burnup: 30 GWd/t). ●: this work; ——: undoped UO_2 (this work); – – – –: summation rule (Neumann–Kopp's law).

Heat capacity analyses were carried out for simulated FPs-doped UO_2. According to Grønvold et al. [2] and Browning [19], the heat capacity of undoped UO_2 can be classified into the following term below 2000 K: (1) the harmonic term of lattice vibration (C_h), (2) the dilatation term (C_d), (3) the anharmonic term of lattice vibration (C_{ah}), which is nearly proportional to temperature, and (4) the Schottky term (C_{sh}), which may be due to excitation of the $5f^2$ electrons in the U^{4+} ion. Since the temperature region is higher than the Debye temperature of UO_2 and the atom number per mole in each sample is 3 in the measurement atmosphere used in this study, the vibration conditions in simulated soluble FPs-doped UO_2 are similar to those of undoped UO_2. Therefore, the contributions of harmonic and anharmonic terms of lattice vibrations to the heat capacity of simulated soluble FPs-doped UO_2 are similar to those of undoped UO_2, and then the results of undoped UO_2 [2,19] were used for the heat capacity analyses of simulated soluble FPs-doped UO_2. In addition, since the results of thermal expansion data [20] and lattice parameter [21,22] showed insignificant differences between undoped and soluble impurities, the changes of dilatation term by soluble impurities may be negligible. Therefore, the results of heat capacity analyses for undoped UO_2 [19] were used in order to analyze the heat capacities of simulated soluble FPs-doped UO_2.

The excess heat capacity, which is almost equivalent to the Schottky term in the temperature region below 2000 K, is expressed as follows:

$$\text{Excess heat capacity} = C_p - C_h - C_d - C_{ah}. \quad (2)$$

Then Eq. (2) was used to obtain the relationship between the excess heat capacities of simulated soluble FPs-doped UO_2 and the concentration of U^{4+} ions in lattices.

The excess heat capacities of simulated FPs-doped UO_2 vs temperature are shown in Fig. 9. The excess heat capacities of undoped and impurity-doped UO_2 may be caused by the Schottky heat capacities of U^{4+} ions [2,23]. The excess heat capacities of simulated FPs-doped UO_2 vs molar cation concentration, excluding U^{4+} ions, at 800 K are shown in Fig. 10. The excess heat capacities of U_4O_9, which has U^{4+} and U^{5+} ions in the crystal are shown for comparison. The excess heat capacities of simulated FPs-doped UO_2 decrease with increasing molar cation concentration, excluding U^{4+} ions, similar to those of U_4O_9. This suggests that the

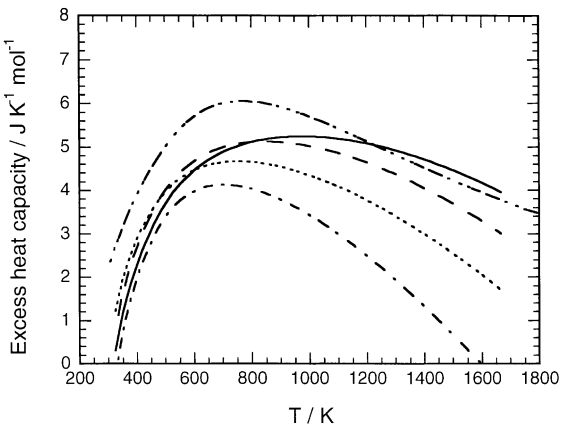

Fig. 9. Excess heat capacities of simulated FPs-doped UO_2. ——: undoped; – – – – – –: simulated burnup: 30 GWd/t; — · — · —: simulated burnup: 90 GWd/t; .....: simulated burnup: 30 GWd/t (6 wt%Gd_2O_3-doped); — · · — · ·: theoretical values [2].

Table 3
Coefficients evaluated from Eq. (1) for each unirradiated sample

Sample no.	Simulated burnup (GWd/t)	Gd_2O_3 content (at.%)	a	b ($\times 10^{-3}$)	c ($\times 10^{6}$)
1	0	0	78.2	7.30	−1.76
2	30	0	79.1	6.19	−1.77
3	90	0	80.8	3.12	−1.95
4	30	8.72	79.2	5.30	−1.71

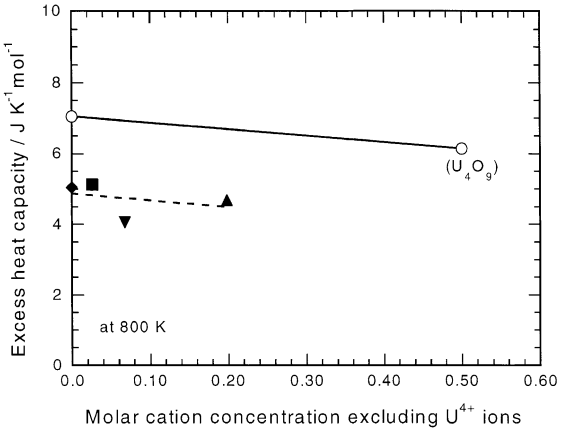

Fig. 10. Relationship between excess heat capacity and molar cation concentration, excluding U^{4+} ions. ◆: undoped; ■: simulated burnup: 30 GWd/t; ▼: simulated burnup: 90 GWd/t; ▲: simulated burnup: 30 GWd/t (6 wt% Gd_2O_3-doped); – – – –: linear regression of this study; — ○ —: Inaba [23].

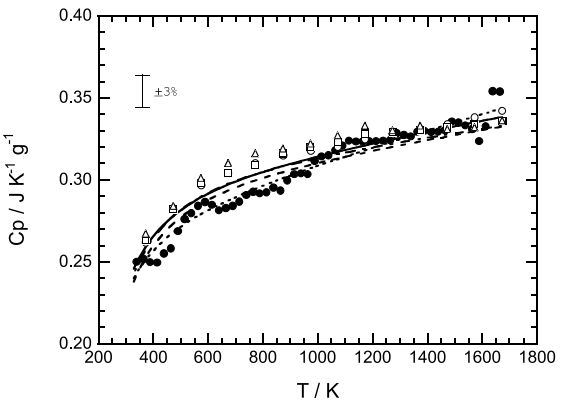

Fig. 11. Heat capacities of UO_2 pellet irradiated in a test reactor (sample No. D14). ●: measurement values (second run); ○: Matzke et al. (unirradiated UO_2) [27]; □: Matzke et al. (3 at.% SIMFUEL) [27]; △: Matzke et al. (8 at.% SIMFUEL) [27]; .....: fitting line of measurement values (second run); —·—·: simulated soluble FPs-doped UO_2 (simulated burnup: 30 GWd/t); – – – –: unirradiated UO_2 (undoped, this work); ——: unirradiated UO_2 [1].

contributions of U^{4+} ions to the heat capacities decrease for simulated soluble FPs-doped UO_2 pellets.

3.2. Heat capacities of irradiated fuel pellets

Using the developed heat capacity measurement technique for microsamples, the heat capacities were measured for fuel pellets irradiated in a test reactor. An example of specific heat capacities of an irradiated fuel pellet (sample No. D14), which are the measured values in the second run measurement is shown in Fig. 11. The sample experienced the temperature up to 1673 K in the first run measurement. In Fig. 11, the heat capacities of unirradiated UO_2 [1], those of simulated soluble FPs-doped UO_2 (simulated burnup: 30 GWd/t) and the literature data of 0%, 3% and 8% SIMFUEL [27] are also shown for comparison.

The heat capacities obtained in the second run measurement agree well with those of unirradiated UO_2, unirradiated simulated FPs-doped UO_2 and the literature data reported by Matzke et al. [27] within the experimental error of this study. This tendency corresponds well with the thermal conductivity changes in irradiated fuel pellets annealed above 1473 K [24,25]. From other post-irradiation examination data for irradiated fuel pellets [26], the irradiation-induced defects such as point defects in irradiated fuel pellets are considered to be recovered completely after the samples are annealed at the temperature above 1273 K. Therefore, the effects of irradiation-induced defects on the measured specific heat capacities of the second run may have mostly disappeared. The measured specific heat capacities of other irradiated fuel pellets have similar tendencies in the second run measurement to those of the irradiated UO_2 pellet as described above. These facts show that the developed heat capacity measurement technique is effective for irradiated fuel pellets having microsample size.

Fission gas releases from the sample were also measured during the heat capacity measurement. The fission gas releases were not observed clearly in the second run measurement.

4. Conclusion

Heat capacities of unirradiated and irradiated fuel pellets were measured by using a DSC in the temperature region from 325 to 1673 K.

For unirradiated fuel pellets, the molar heat capacities of simulated soluble FPs-doped UO_2 having burnups up to 90 GWd/t were close to those of undoped UO_2, and heat capacity anomalies were not observed above 1000 K, which was in contrast with the results reported by Arita et al. The heat capacity analysis was carried out for simulated FPs-doped UO_2 and the relationship between the excess heat capacities of simulated soluble FPs-doped UO_2, and the concentration of U^{4+} ions in the lattices was obtained. The excess heat capacities of simulated FPs-doped UO_2 decreased with increasing molar cation concentration, excluding U^{4+} ions. This suggests that the contributions of U^{4+} ions to the heat capacities decreased for simulated soluble FPs-doped UO_2.

A heat capacity measurement technique was developed for irradiated fuel pellets. From the heat capacity

measurement results of an α-Al_2O_3 sample (square with a 2.5 mm side and 0.75 mm thickness), it was shown that the developed technique was effective for measuring the heat capacity of small samples. The measurement technique was used to obtain heat capacities of fuel pellets, which had been irradiated at isothermal conditions in a test reactor. In the second run measurement, the heat capacities were nearly equal to those of unirradiated UO_2 and unirradiated simulated FPs-doped UO_2.

Acknowledgements

This work was carried out as a joint study by the JAERI (Japan Atomic Energy Research Institute) – NFD (Nippon Nuclear Fuel Co., Ltd.). The authors would like to express their gratitude to Mr H. Masuda for preparation of unirradiated samples. They also thank Dr S. Kashibe, Mr K. Matsushima and Mr H. Uchikoshi for experimental supports on irradiated samples.

References

[1] D.L. Hagrman, G.A. Reymann (Eds.), TREE-NUREG-CR-0497, 1979.
[2] F. Grønvold, N. Jørgen Kveseth, A. Sveen, J. Tichy, J. Chem. Thermodyn. 2 (1970) 655.
[3] J.F. Kerrisk, D.G. Clifton, Nucl. Technol. 16 (1972) 531.
[4] D.R. Fredrickson, M.G. Chasanov, J. Chem Thermodyn. 2 (1970) 623.
[5] R.A. Hein, P.N. Flagella, J.B. Conway, J. Am. Ceram. Soc. 51 (1968) 291.
[6] H. Inaba, K. Naito, M. Oguma, J. Nucl. Mater. 149 (1987) 341.
[7] Y. Takahashi, M. Asou, J. Nucl. Mater. 201 (1993) 108.
[8] Y. Takahashi, M. Asou, Thermochim. Acta. 223 (1993) 7.
[9] Y. Takahashi, M. Asou, S. Shimizu, N. Okamoto, T. Terai, in: Proc. 1991 Fall Mtg. Japan Atom. Energ. Soc. G56, 1991, p. 466.
[10] Y. Kosaka, S. Doi, in: Proc. 1991 Fall Mtg. Japan Atom. Energ. Soc. G55, 1991, p. 465.
[11] Y. Arita, S. Hamada, T. Matsui, Thermochim. Acta. 247 (1994) 225.
[12] T. Matsui, Y. Arita, K. Naito, J. Nucl. Mater. 188 (1992) 205.
[13] Y. Arita, T. Matsui, S. Hamada, Thermochim. Acta. 253 (1995) 1.
[14] P.G. Lucuta, Hj. Matzke, R.A. Verrall, H.A. Tasman, J. Nucl. Mater. 188 (1992) 198.
[15] R.A. Verrall, P.G. Lucuta, J. Nucl. Mater. 228 (1996) 251.
[16] R.A. Gomme, J.C. Carrol, T.L. Shaw, High Temp. – High Press. 30 (1998) 135.
[17] D.G. Archer, J. Phys. Chem. Ref. Data. 22 (1993) 1441.
[18] I. Barin (Ed.), Thermochemical Data for Pure Substances, VCH, Weinheim, Germany, 1989.
[19] P. Browning, J. Nucl. Mater. 98 (1981) 345.
[20] K. Une, J. Nucl. Sci. Technol. 23 (1986) 1020.
[21] K. Une, M. Oguma, J. Nucl. Mater. 131 (1985) 88.
[22] T. Ohmichi, S. Fukushima, A. Maeda, H. Watanabe, J. Nucl. Mater. 102 (1981) 40.
[23] H. Inaba, Netsu-sokutei 12 (1985) 30 in Japanese.
[24] M. Amaya, M. Hirai, H. Sakurai, K. Ito, M. Sasaki, T. Nomata, K. Kamimura, R. Iwasaki, in: Proc. IAEA TCM Nucl. Fuel Behavior Model. High Burnup Experiment. Support, Session No. 1-1, 18–23 June, Winderemere, UK, 2000.
[25] K. Minato, T. Shiratori, H. Serizawa, K. Hayashi, K. Une, K. Nogita, M. Hirai, M. Amaya, J. Nucl. Mater. 288 (2001) 57.
[26] K. Nogita, K. Une, J. Nucl. Sci. Technol. 30 (1993) 900.
[27] Hj. Matzke, P.G. Lucuta, R.A. Verrall, J. Henderson, J. Nucl. Mater. 247 (1997) 121.